

11th International Symposium on Plasticity and Impact Mechanics, Implast 2016

# Lip Formation and Ejecta from LPSO-type Magnesium Alloy Plates in Hypervelocity Impact

Masahiro Nishida<sup>a,\*</sup>, Kaito Ishida<sup>a</sup>, Fumiya Kodama<sup>a</sup>, Koichi Hayashi<sup>b</sup>,  
Yasuhiro Akahoshi<sup>c</sup>, Kazuyuki Hokamoto<sup>d</sup>, Yoshihito Kawamura<sup>d</sup>

<sup>a</sup>*Nagoya Institute of Technology, Gokiso-cho, Showa-ku, Nagoya, Aichi 466-8555, Japan*

<sup>b</sup>*National Institute of Technology, Toba College, 1-1, Ikegami-cho, Toba City, Mie, 517-8501, Japan*

<sup>c</sup>*Kyushu Institute of Technology, 1-1 Sensui-cho, Tobata-ku, Kitakyushu-shi, Fukuoka, 804-8550, Japan*

<sup>d</sup>*Kumamoto University, 2-39-1 Kurokami, Chuo-ku, Kumamoto 860-8555, Japan*

---

## Abstract

Long period stacking ordered (LPSO) type magnesium alloys have the low density, excellent mechanical strength and ignition resistance. LPSO-type magnesium alloys have a great potential as structural materials of satellites. Lip formation and ejecta size were examined when spherical projectiles strikes thin plates made of LPSO-type magnesium alloy at hypervelocities of 5 km/s. Witness plates were placed in front of and behind each target to determine the scattering area. After impact experiments, ejecta were collected from test chamber and lips near penetration hole was examined x-ray computed tomography (CT) in detail. Results of LPSO-type magnesium alloy plates were compared with those of aluminum alloy (A6061-T6). Images of scattering ejecta taken by a high speed video camera were also discussed.

© 2017 The Authors. Published by Elsevier Ltd. This is an open access article under the CC BY-NC-ND license (<http://creativecommons.org/licenses/by-nc-nd/4.0/>).

Peer-review under responsibility of the organizing committee of Implast 2016

**Keywords:** Hypervelocity, Ejecta, Magnesium alloy, Plate target, Space debris;

---

## 1. Introduction

Micrometeoroids and orbital debris (MMOD) often strike space stations and spacecraft at very high velocities. The International Space Station employs shields, such as the Whipple shield and the staffed Whipple shield, which consist of thin plates to protect itself from MMOD. When MMOD perforates thin plates, debris clouds are formed. In such a case, a part of projectile and target materials are ejected in the reverse direction at almost the same time as the growth of the debris clouds. Fragments ejected from the target surface and fragmented projectile are scattered widely. These ejecta and fragments have the potential to become orbital debris (known as secondary debris).

Aluminum alloys have been used as structural materials of space stations and satellites. Kawamura et al. have developed magnesium alloys with long period stacking ordered (LPSO) phase [1]. LPSO-type magnesium alloys have excellent mechanical strength and ignition resistance. LPSO-type magnesium alloys have great potential as structural materials of space stations and satellites. We examined lip formation and ejecta size when spherical projectiles strikes thin plates made of LPSO-type magnesium alloy, Mg<sub>95.65</sub>Zn<sub>2</sub>Y<sub>2</sub>La<sub>0.1</sub>Al<sub>0.25</sub> (at.%), at hypervelocities of 5 km/s. Results of LPSO-type magnesium alloy plates were compared with those of aluminum alloy (A6061-T6).

## 2. Experimental Methods

Projectiles were made of aluminum alloy 2017-T4 with a diameter of 1.0 mm based on ISO 11227 [2]. Two-stage light gas guns at Japan Aerospace Exploration Agency, (JAXA) was used for impact test [3]. The impact velocity was 5.0 km/s. Plates of LPSO-type magnesium alloy, Mg<sub>95.65</sub>Zn<sub>2</sub>Y<sub>2</sub>La<sub>0.1</sub>Al<sub>0.25</sub> (at. %) (Fuji Light Metal Co.) [4-6], were used as targets. In order to compare results, aluminum alloy, A6061-T6, was also used as target materials. Target size was 150 mm in length, 50 mm in width. The thickness of the magnesium alloy was 1.5 mm and the aluminum alloy 1.0 mm because the thickness was chosen so that the areal density was almost the same. The density of the magnesium alloy is 1.89 g/cm<sup>3</sup> and the aluminum alloy 2.70 g/cm<sup>3</sup>, based on ISO11227. Front and rear witness plates (200 mm × 200 mm, 2 mm in thickness) made of copper, C1100P-1/4H, were placed 50 mm in front of and behind each target as shown in Fig. 1 to determine the scattering area and the number of ejecta. Front witness plates have a hole of 25 mm through which the projectile could pass. When the forward ejecta and backward ejecta coming from the target were separately collected, space between the target and the rear witness plate was surrounded by plates. After impact experiments, the length of ejecta collected from test chamber was measured using image analysis software (ImageJ). The ejecta debris immediately after impact was observed using a high-speed video camera (Shimadzu, HPV-X).

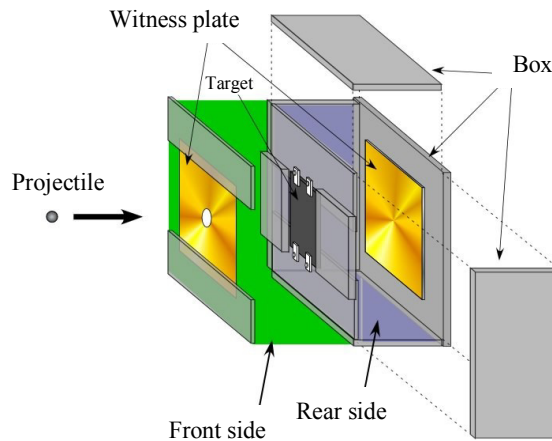


Fig. 1. Experimental setup for hypervelocity impact.

## 3. Results and Discussion

### 3.1. Observation of targets

Fig. 2 shows photographs of penetration holes after impact tests. Fig. 2(a) shows that lips on the impact side and the rear side are developed near the penetration hole of aluminum alloy plates. The LPSO-type Mg plate does not have large lips on the front side and the rear side. Rough surfaces are observed near the penetration hole of LPSO-type Mg.

Fig. 3 shows images near penetration holes taken by X-ray computed tomography (X-ray CT: Shimadzu, inspeXio SMX-100CT). The cross-section images also show that the aluminum alloy plate has large lips and the

LPSO-type Mg plate does not have large lips. The LPSO-type Mg plate near the penetration hole is split off in the thickness direction and many cracks are observed. The longitudinal direction of specimens is the extruded direction of extruded rods and the thickness direction and width direction of specimens are perpendicular to extruded direction. The mechanical properties of specimens in the longitudinal direction are greater than that in the thickness direction [4, 7]. Because of anisotropy, it seems that many cracks in the longitudinal direction which is perpendicular to the thickness direction are additionally observed.

Based on the definition of crater area and lip area shown in Fig. 4, the volumes of crater area and lip area were measured using software for three dimensional computer tomography (CT) data analysis, VGstudio MAX2.2 (Volume Graphics GmbH). Table 1 shows that the crater volume of LPSO-type Mg is three times larger than that of Al 6061-T6, even though the thickness of LPSO-type Mg is 1.5 times larger than that of Al 6061-T6. Next, the ejecta volume and mass from plates was estimated by the volume of crater area and lip area. When the decrease in volume is calculated using the difference in volume between the crater area and lip area, the change in volume of LSPO-type Mg was 5.5 times larger than that of Al 6061-T6. In the case of Al 6061-T6, the ratio of lip volume to crater volume is large which means that large lips are developed. It is expected that ejecta of Al 6061-T6 is less because of large developed lips. Because the difference between crater volume and lip volume is closely related with ejecta from target, the mass change is calculated using the volume change and the densities of the magnesium alloy,  $1.89 \text{ g/cm}^3$ , and the aluminum alloy,  $2.70 \text{ g/cm}^3$ . The mass decrease of LPSO-type Mg is 3.8 times greater than that of Al 6061-T6. Next, Table 2 shows change in measured mass of target before and after experiments. The mass decrease of LPSO-Mg is 3.8 times larger than that of Al 6061-T6. The measured mass decrease of LPSO-Mg is 40.2 mg whereas the calculated mass decrease using volume change is 54.0 mg. The ratio of LPSO-Mg to Al 6061-T6 is the same in both cases. However, the absolute value in both cases is not the same and the ratio was 1.3.

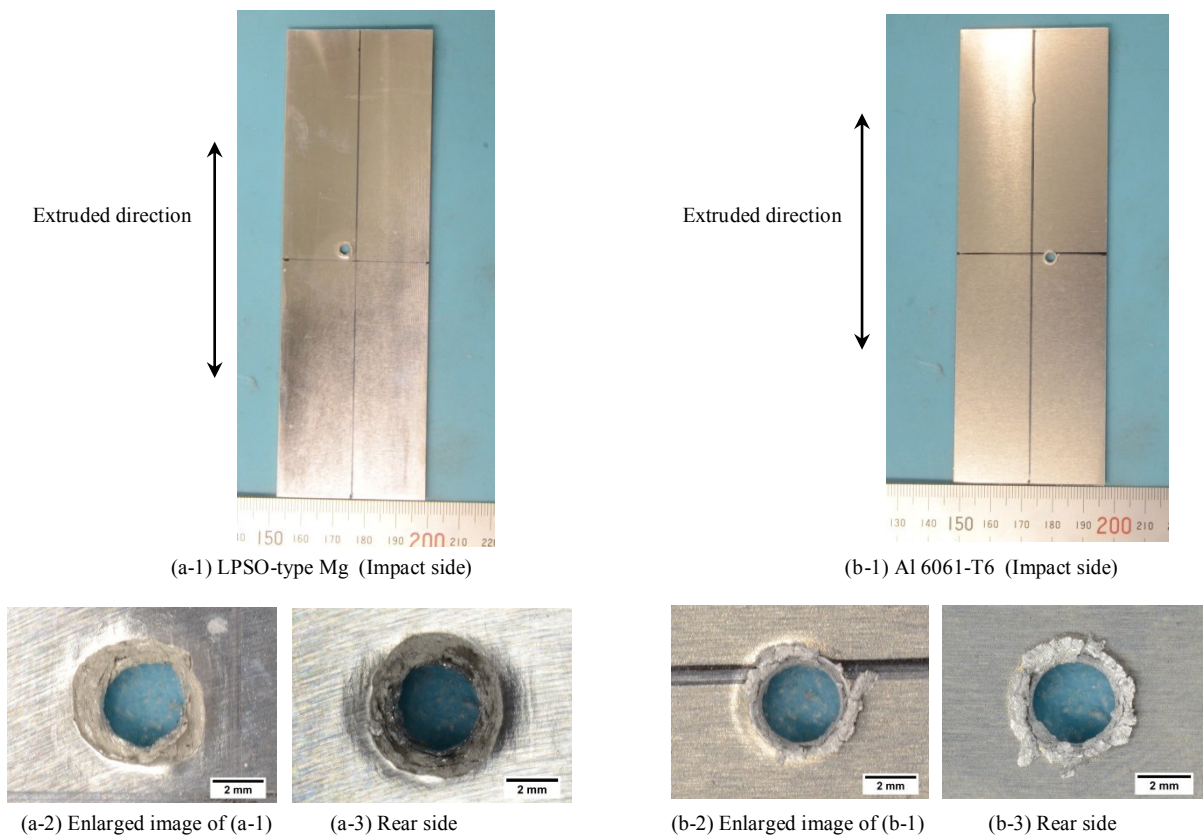


Fig. 2. Penetration holes of LPSO-type Mg (5.29 km/s) and Al (5.16 km/s).

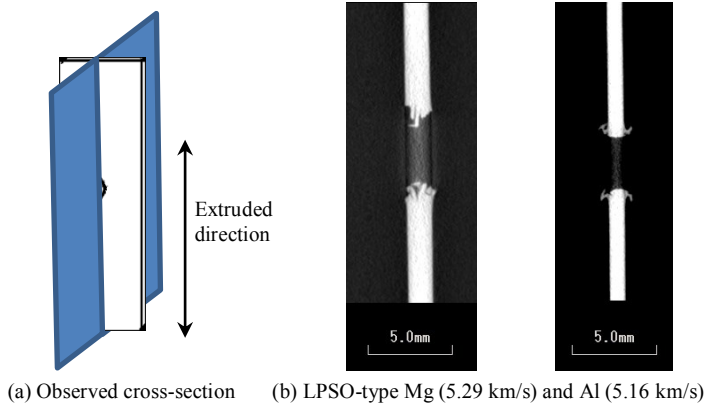


Fig. 3. Images of cross-section taken by X-ray CT.

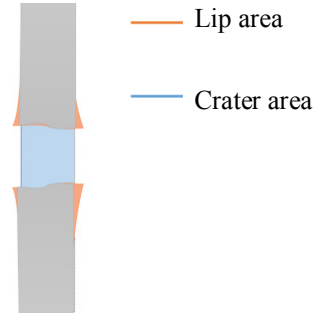


Fig. 4. Definition of lip area and crater area.

Table 1. Crater volume and lip volume.

	LPSO-Mg	A6061-T6
Crater volume, mm <sup>3</sup>	30.68	8.39
Lip volume, mm <sup>3</sup>	1.48	3.06
Difference in volume between crater and lip, mm <sup>3</sup>	29.20	5.33
Estimated mass of ejecta, mg	54	14

Table 2. Change in target mass measured by electric balance.

	LPSO-Mg	A6061-T6
Target mass before impact tests, g	20.45818	19.76542
Target mass after impact tests, g	20.41796	19.75503
Difference, mg	40.22	10.39

Table 3. Collection rate and mass of ejecta collected from test chamber.

	Ejecta mass on front side, mg	Ejecta mass on rear side, mg	Total ejecta mass, mg	Collection rate, %
LPSO-type Mg	18.18	19.05	37.23	92.6
A6061-T6	2.52	4.67	7.19	69.2

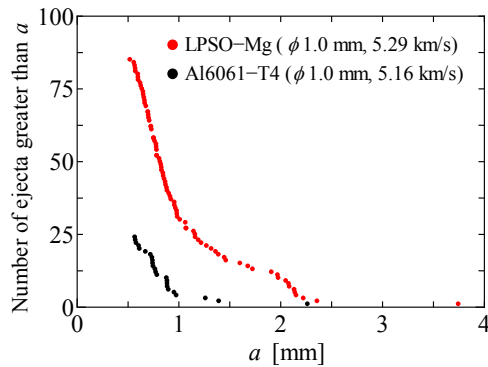


Fig. 5. Cumulative number distribution of ejecta size  $a$ .

### 3.2. Ejecta collected from test chamber

Table 3 shows ejecta mass on the front side of target, ejecta mass on the rear side of target and the collection rate. Ejecta mass of LPSO-type Mg collected from test chamber is greater than that of Al 6061-T6. The collection rate of LPSO-type Mg is over 90%. In the case of LPSO-type Mg plate, ejecta mass on the front side and rear side are almost the same. In the case of Al6061-T6, ejecta mass on the rear side is greater than that of front side. The collection rate of Al6061-T6 was near 70%.

After a photograph of each ejecta was taken, ejecta size was measured using image analysis software, ImageJ. The cumulative number of ejecta length,  $a$ , on the front side is shown in Fig. 5. In this figure, the cumulative number of ejecta length on the vertical axis means the number of ejecta with a length greater than the length of ejecta on the horizontal axis. When ejecta with a length over 0.5 mm are compared, the maximum length and the cumulative number of LPSO-type Mg are greater than those of Al 6061-T6. It seems that the cumulative number of LPSO-type Mg and Al 6061-T6 suddenly increases at an ejecta length of 1.0 mm.

The length,  $a$ , of ejecta collected from test chamber was also measured by the scan system and scan method as shown in Fig. 6. In Fig. 7, the cumulative number of ejecta of LPSO-type Mg is greater than that of Al 6061-T6 on both the front side and rear side. In the range of less than 0.1 mm, the cumulative number of ejecta of LPSO-type Mg and Al 6061-T6 is the same. With respect to large ejecta, the trend of Fig. 7 is similar to the results of Fig. 5.

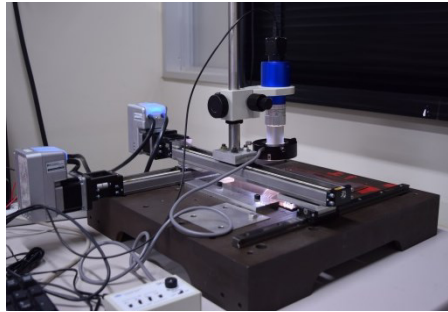


Fig. 6. Photograph of scan system.

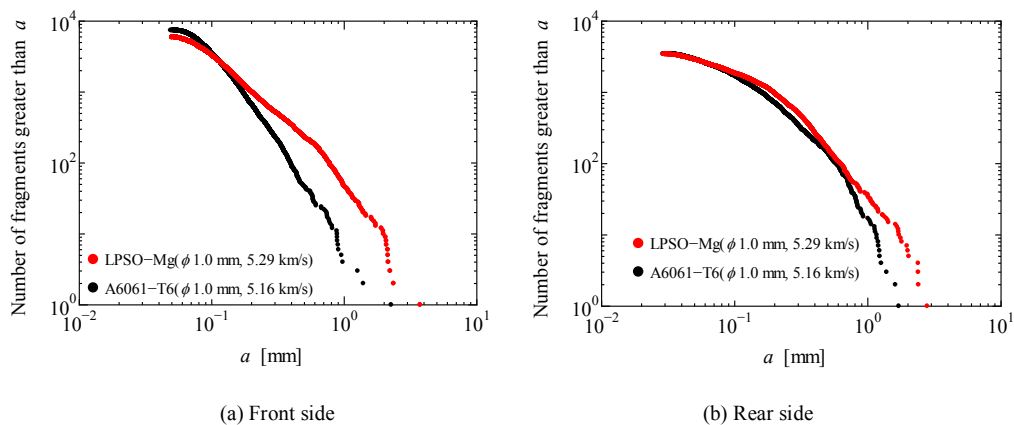


Fig. 7. Distribution of ejecta size  $a$  measured by scan system.

### 3.3. Analysis of witness plates

Fig. 8 shows photographs of witness plates after impact tests. Fig. 9 shows results after image analysis of the witness plates using scanned images. On the front side, a clear ring with radial lines consisting of ejecta impact craters is observed on the witness plate of Al 6061-T6, whereas ejecta impact craters of LPSO-type Mg is heavily concentrated in a central circle. On the rear side, ejecta impact craters in a large circle are observed in both cases and many smaller ejecta impact craters are clearly observed only on the witness plate of LPSO-type Mg.

Next, the number distribution of the ejecta impact craters using image analysis of the witness plates is examined based on ISO 11227. The cumulative number distributions of crater diameter are shown in Fig. 10. On the front side, the number distributions of the ejecta impact craters over a diameter of 0.3 mm are almost the same in both cases, whereas there are many ejecta impact craters less than 0.3 mm when the LPSO-type Mg plate is used. Fig. 5 and 7(a) show that the cumulative number of ejecta collected from LPSO-type Mg plates is greater than that of Al6061-T6. The trend of Fig. 10 is different from those of Fig. 5 and 7(a). The large ejecta do not affect results of ejecta impact craters on the witness plate. On the rear side of witness, the number distributions of the ejecta impact craters over a diameter of 0.1 mm are almost the same in both cases. This means that defense properties as space debris bumpers are almost the same of LPSO-type Mg and Al6061-T6. Fig. 11 shows enlarged images of rear side witness plates. In the case of LPSO-type Mg, many small craters are dense. This observation is in consistency with the results of Fig. 10.

Finally, Fig. 12 shows that observed ejecta from LPSO-type Mg were more than that from Al 6061-T6 and ejection duration of LPSO-type Mg is longer than that of Al 6061-T6. Because large craters are not observed on witness plate in the case of Al 6061-T6, it is expected that scattering velocity of ejecta from A6061-T6 is low. It is highly possible that ejecta formation mechanisms are different between LPSO-type Mg and Al 6061-T6.

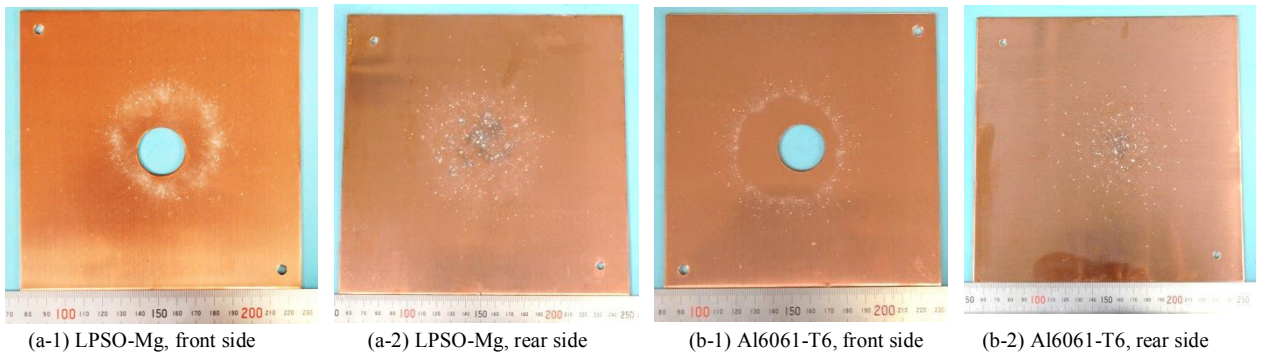


Fig. 8. Photographs of witness plates after impact tests.

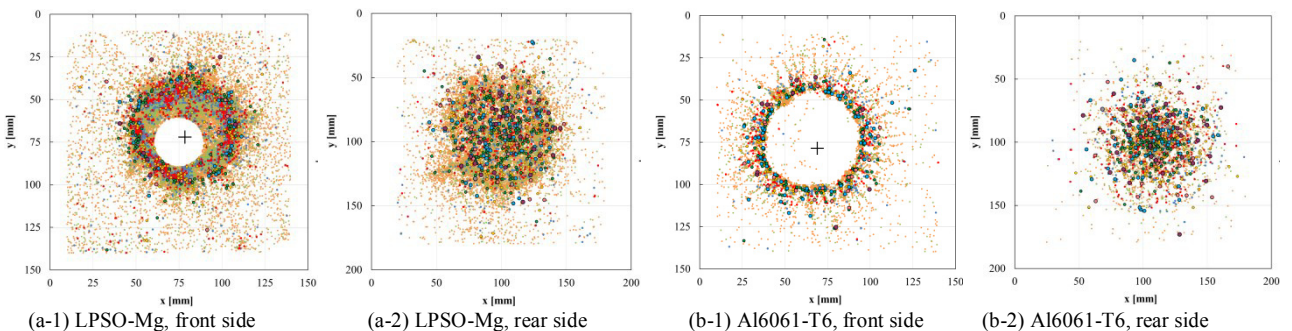


Fig. 9. Results after image analysis of the witness plates.

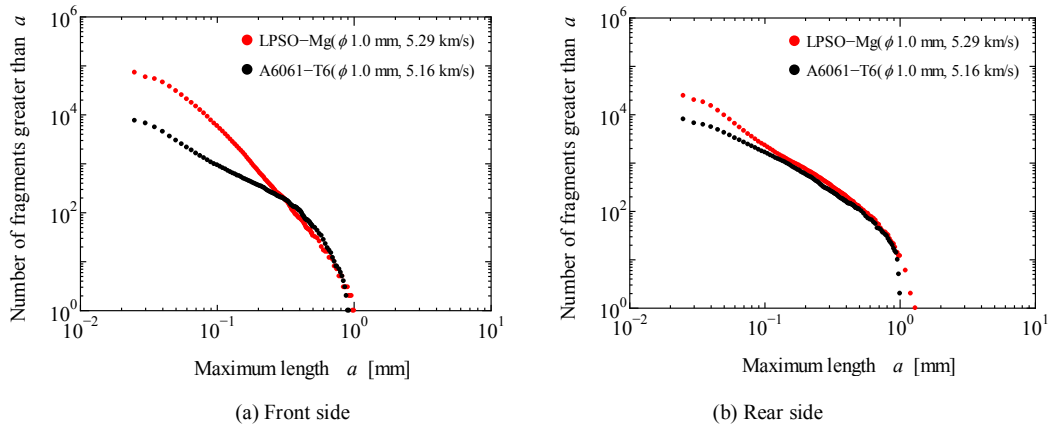


Fig. 10. Cumulative number distribution of crater diameter on witness plate.

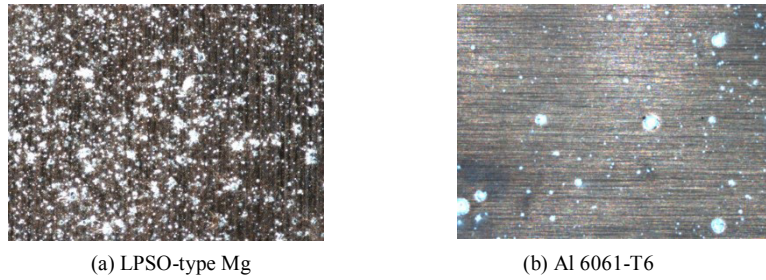


Fig. 11 Enlarged images of witness plates, rear side.

